C. R. Mecanique 341 (2013) 15–25

Contents lists available at SciVerse ScienceDirect

Comptes Rendus Mecanique

www.sciencedirect.com

Combustion, flow and spray dynamics for aerospace propulsion

Numerical simulation of primary and secondary atomization

Davide Zuzio *, Jean-Luc Estivalezes, Philippe Villedieu, Ghislain Blanchard

ONERA (The French Aerospace Lab), 2, avenue Edouard-Belin, 31055 Toulouse cedex 4, France

ARTICLE INFO

Article history:
Available online 8 January 2013

Keywords:
Combustion
Primary and secondary atomization
Multi-phase flows
Direct numerical simulation
Sharp interface methods
Diffuse interface methods
Dispersed phase methods

ABSTRACT

The physics of the atomization process involves many complex phenomena, which occur at different scales of space and time. The numerical study of such a problem is a great challenge for different reasons. Large density ratios, presence of a singular surface tension force, interface localization and transport, mass conservation, all of these make accurate numerical simulation difficult to perform. Several strategies have been investigated at ONERA in order to find an optimal method to simulate the atomization process with the CEDRE code. Both interface capturing and diffuse interface algorithms have been tested. The present development consists in the implementation of a multi-fluid version of the current gas solver of CEDRE, which conserves all its original features. One of the principal axes of research is based on a method which couples the new multi-fluid method with one of the dispersed phase solvers of CEDRE. The long term purpose is to be able to perform numerical simulation of both primary and secondary atomization.

1. Introduction

In the vast topic of flows with interfaces, the study of liquid–gas interactions has a fundamental importance, especially in combustion problems. The most common injectors found in aeronautical engines, called *airblast* atomizers, use the assisted atomization to pulverize the fuel in order to maximize the liquid surface and improve the combustion efficiency. The assisted atomization process can be described as the ensemble of mechanisms which occur in the injection of a high pressurized liquid through a small fence (planar or annular) sandwiched by airflows, and its effect on the configuration of the liquid sheet.

Two different stages can be distinguished in this process. The first involves the region near the orifice (some diameters/thickness from the injector) where the primary atomization takes place. Here the sheet becomes subject to longitudinal instabilities, which are the results of the shearing effect triggered by the interaction between the liquid and gas flows: Kelvin–Helmholtz instabilities perturb the plane sheet starting a sinusoidal stream-wise oscillation, which manifests itself all along the sheet. This is called the global oscillation: the sheet waves inside and outside the gas flow like a flag in the wind. The following instability involves the third dimension, and manifests itself as a transverse modulation. The sheet breaks into smaller liquid packs, ligaments and bag-like structures, which are in turn affected by the shearing effect of the air flow. This continuous fragmentation in smaller and smaller structures is the secondary atomization, a mechanism which ends with the formation of a spray of droplets. The droplets broken-off from the liquid sheet are reported in experiments to be as much as ten times smaller than its diameter, as in [1–3].

Numerical simulations of the atomization processes have become possible thanks to sharp-interface-tracking algorithm. Three-dimensional DNS simulations of liquid jet breakup have been reported in [4,5], while in [6–8] a full assisted

* Corresponding author.
E-mail addresses: davide.zuzio@onera.fr (D. Zuzio), jean-luc.estivalezes@onera.fr (J.-L. Estivalezes), philippe.villedieu@onera.fr (P. Villedieu), Ghislain.Blanchard@onera.fr (G. Blanchard).

1631-0721/$ – see front matter
http://dx.doi.org/10.1016/j.crme.2012.10.003

atomization is simulated in different configurations. The secondary atomization is often modelled by stochastic approaches as in [9,10], or directly by Lagrangian models. A more general approach consists in coupling different solvers to get the best of both worlds, as in [11,12], where a coupled DNS and Lagrangian method simulate different moments of atomization.

In this paper a review of the numerical methods used at ONERA to simulate atomization is presented, as well as the development of a new hybrid solver which will be integrated in the ONERA CEDRE code. The article is organized as follows: the first part is an overview of the numerical methods developed at ONERA to simulate primary atomization, with some significant test cases, two and three dimensional; the second part is the preliminary work about a new hybrid solver aimed to perform simulation of primary and secondary atomization.

2. Numerical methods for simulating atomization

No numerical model is satisfying in simulating the whole process, as several difficulties arise: the multi-scale nature of the problem, where many orders of magnitudes separate the largest from the smallest scales in space and time; the steep variations of the physical quantities, as density of the fluid; the modelling of the interface separating the fluids and its localized surface tension force; the mass conservation of each fluid. Moreover, in order to make statistics several cycles of the phenomena should be followed, which means long simulation times.

Looking at the phenomena involved in primary and secondary atomization, two numerical approaches seem suitable:

- ▹ The interfacial flow approach. In this case each phase occupies its own part of the domain; the Navier–Stokes equations are solved independently in each phase, while in the separation zone (the interface) the stress tensor jump imposes the boundary conditions for each phase.
- ▹ The dispersed phase approach. In this case one phase, which occupies the whole domain, is considered as continuous and usually follows the Navier–Stokes equations. The second phase can be dispersed in discrete points (Lagrangian approach) or can be modelled by a discrete concentration function (Eulerian approach), its motion being determined by the transport equations of the continuous flow.

For the primary atomization problem, the first approach is more appropriate because of the initial clear separation of the two fluids, while the second method class is more oriented towards the simulation of a set of particles being transported by the flow: it is, for this reason, more suitable to follow the droplet cloud formed during the atomization process, and to simulate the vaporization and combustion processes. The development of a hybrid solver may become an optimal choice.

2.1. State of the art at ONERA

Within the interfacial flow methods, two main approaches to multi-phase flows have been investigated at ONERA. The first (DYJEAT, [13]) is an incompressible parallel sharp interface code, which relies upon the Level-Set/Ghost-Fluid method on structured Cartesian meshes, and was explicitly designed for primary atomization. The second (SLOSH, [14]) is a low Mach compressible diffuse interface method working on unstructured meshes, which was developed to reproduce tank sloshing phenomena in zero gravity environments, and recently tested on the same configurations as DYJEAT.

The purpose of the DYJEAT code within the ONERA atomization project is to perform high resolution simulations, which can be used as reference solutions and as “calibration” tools for atomization models. On the other hand, the atomization investigation needs a more “industrial” tool, which should be faster, more flexible, capable to be coupled with other solvers (multi-physics simulations) and to work with realistic parameters and configurations (real injectors), as well as to deal with more complex flows (more than two phases). The aim of the hybrid solver project is to get such a tool, and the ONERA multi-physics CEDRE (http://cedre.onera.fr/) platform seems the ideal candidate. The hybrid solver should couple two methods appropriate for the simulation of respectively primary and secondary atomization. The first, acting on the small region close to the injector, should be based on an Eulerian multi-fluid formulation, as the liquid phase is dense and the interface topology complex. The second, which has to work on the rest of the domain, should handle a dispersed phase (a droplet cloud), and potentially evaporation and combustion processes, either in Eulerian or Lagrangian way.

The development of the new solver is realized on the SLOSH code, because of the many characteristics in common with the CEDRE fluid solver: the unstructured finite volume approach, the four-equation model (mechanical and thermal equilibrium within the cell), the mass conservation of each component of the numerical mix, the compressible formulation. Moreover, the diffuse interface model is theoretically able to deal with an arbitrary number of fluids (in contrast with the two-fluid only Level-Set method). The comparison between the DYJEAT and SLOSH results can reveal much about the possibility to perform atomization simulations with a diffuse interface formulation. In addition, the SLOSH code has been optimized to work in low-Mach regimes [15], and its numerical schemes are well suited candidates for the implementation within CEDRE.

2.1.1. The DYJEAT code

The DYJEAT code performs direct numerical simulation (as far as the mesh size allows) of two-phase flows, using an interface capture method: the interface location and topology is known over time. The mesh is a Cartesian staggered MAC. The DYJEAT two phase model consists in the incompressible Navier–Stokes equations solved in each of the two fluids. The

computational domain is divided in the corresponding two regions separated by a sharp interface. In each of them the model is:

$$\begin{cases} \nabla \cdot \boldsymbol{u} = 0 \\ \dfrac{\partial \boldsymbol{u}}{\partial t} + (\nabla.\boldsymbol{u})\boldsymbol{u} = \dfrac{1}{\rho}\big(\nabla \cdot \big(-p\mathbf{I} + \mu\big(\nabla \boldsymbol{u} + (\nabla \boldsymbol{u})^T\big)\big) + f\big) \end{cases} \tag{1}$$

where $\boldsymbol{u} = [u, v]$ represents the velocity vector field, p the hydrodynamic pressure, ρ the density, μ the dynamic viscosity of the fluid and f the external forces like gravity. The Level-Set function, of which the zero iso-contour represents the interface, is a scalar function passively advected by the flow

$$\frac{\partial \phi}{\partial t} + \boldsymbol{u}.\nabla\phi = 0 \tag{2}$$

Across the interface, the jump conditions are imposed by capillarity and viscosity; the velocity respects a no-slip condition:

$$\begin{cases} [p] - \boldsymbol{n}.\big[\mu\big(\nabla \boldsymbol{u} + (\nabla \boldsymbol{u})^T\big)\big].\boldsymbol{n} = \sigma\kappa \\ \boldsymbol{t}.\big[\mu\big(\nabla \boldsymbol{u} + (\nabla \boldsymbol{u})^T\big)\big].\boldsymbol{n} = 0 \\ [\boldsymbol{u}] = 0 \end{cases} \tag{3}$$

Here the notation $[\cdot] = (\cdot)_1 - (\cdot)_2$ represents the jump across the interface, $\boldsymbol{n}$ the normal vector pointing from 1 to 2, t the tangential one. σ is the surface tension, κ the interface curvature. The numerical method used to solve the system (1) is a projection method. High order WENO schemes are employed for the discretization of the spatial derivatives of both the Level-Set function and the velocities. The advection equation (2) is integrated in time by an accurate three step Runge–Kutta scheme, while Eq. (1) uses an Adams–Bashford algorithm. The elliptic equation from the projection method is solved by a fast multigrid preconditioned conjugate gradient method. An oct-tree adaptive mesh refinement variant of the code has been developed as well [16]. It supports parallel decomposition of the domain.

2.1.2. The SLOSH code

The SLOSH code is based on a two-fluid formulation, in which both fluids are supposed to be simultaneously present at any given point, while a compressible equation of state is given for both the gas and the liquid. There is no explicit interface, nor any reconstruction is needed for computational purposes. A guess of the interface location is given by the 0.5 value iso-contour of the liquid (or gas) volume fraction. If needed, reconstruction procedures similar to those used in VOF formulations can be employed. The model is based on mass balance equations for the two fluids and a momentum equation for the numerical mixture. The mass conservation equations writes:

$$\frac{\partial \tilde{\rho}_i}{\partial t} + \nabla.(\tilde{\rho}_i \boldsymbol{u}) = 0 \tag{4}$$

where $\boldsymbol{u}$ is the mixture velocity and $\tilde{\rho}_i = \alpha_i \rho_i$, with α_i the volume fraction of fluid i and ρ_i its bulk density. The mixture momentum equation reads:

$$\frac{\partial \rho \boldsymbol{u}}{\partial t} + \nabla.(\rho \boldsymbol{u} \otimes \boldsymbol{u} + p\mathbf{I}) = \nabla.(\tau_v + \tau_c) + \rho \mathbf{g} \tag{5}$$

where $\rho = \tilde{\rho}_1 + \tilde{\rho}_2$ is the mixture density, p the mixture pressure, τ_v the viscous stress tensor, τ_c the capillary stress tensor and $\mathbf{g}$ the gravity acceleration. Details of the model and the expression of τ_v and τ_c are found in [17] and [15].

The problem is to choose an equation of state for the virtual mixture which correctly degenerates when only one fluid is present locally. The local pressure equilibrium between the two fluids allows to respect this constraint, and yields:

$$p(\tilde{\rho}_1, \tilde{\rho}_2) = p_1\left(\frac{\tilde{\rho}_1}{\alpha_1^*}\right) = p_2\left(\frac{\tilde{\rho}_2}{\alpha_2^*}\right) \tag{6}$$

where the volume fractions at equilibrium α_1^* and α_2^* are solutions of the following algebraic system of equations:

$$\begin{cases} \alpha_1^* + \alpha_2^* = 1 \\ p_1\left(\dfrac{\tilde{\rho}_1}{\alpha_1^*}\right) = p_2\left(\dfrac{\tilde{\rho}_2}{\alpha_2^*}\right) \end{cases} \tag{7}$$

The system (7) leads to a single solution if the equations of state of both fluids satisfy the conditions described in [17], where they assume a linearised isothermal form:

$$p_i(\rho_i) = p_0 + c_i^2(\rho_i - \rho_{i,0}) \tag{8}$$

where the quantities $(\cdot)_0$ are reference values. Imposing the equality of the partial pressures $p_1 = p_2$ of the two fluids, which is a necessary condition to make the mathematical system to be hyperbolic, assures the existence of one only solution $0 < \alpha^* < 1$.

2.2. Primary atomization: two dimensional case

The first primary atomization test case is two dimensional. It is designed to capture the global (stream-wise) oscillation of the sheet, for which the two dimensional approximation is acceptable. The test has been carried on both DYJEAT and SLOSH codes, and a qualitative comparison has been made. The physical parameters correspond to an experience realized at the ONERA LACOM laboratory of Fauga-Mauzac, done with 10 bar pressurized air and water.

The test is set up as follows. A square box is defined by three outlet boundary conditions and a wall which presents three injection fences, each of them with a given velocity profile: a liquid flow sheared by two parallel air streams. The mesh is Cartesian uniform in DYJEAT with 256×256 cells, Cartesian non-uniform in SLOSH with 256×223 vertically stretched cells [18]. The velocity profiles are given in the liquid by a laminar Poiseuille profile:

$$u(y) = \frac{3U_l}{2a^2}\left(a^2 - y^2\right) \tag{9}$$

with U_l the mean incoming liquid velocity of 2 $\mathrm{m\,s^{-1}}$. The velocity field of the two parallel flows above and beyond the sheet is defined by a Polhausen fourth order polynomial profile in the boundary layer and a constant profile outside:

$$\frac{u(y)}{U_g} = 2\frac{y}{\delta} - 2\left(\frac{y}{\delta}\right)^2 + \left(\frac{y}{\delta}\right)^4 \tag{10}$$

where $\delta = 300$ µm is the boundary layer thickness near the sheet and $U_g = 30\ \mathrm{m\,s^{-1}}$ the undisturbed velocity. The densities for liquid and gas are respectively $\rho_g = 12.26\ \mathrm{kg\,m^{-3}}$ and $\rho_l = 1000\ \mathrm{kg\,m^{-3}}$ (density ratio of 81.97), the viscosities $\mu_g = 1.78 \times 10^{-3}$ Pa s and $\mu_l = 1.132 \times 10^{-2}$ Pa s (these are about ten times higher than real values, and were raised for stability issues of DYJEAT). The surface tension coefficient is $\sigma = 7.28\ \mathrm{N\,m^{-2}}$. The momentum ratio M is 2.16.

2.2.1. Qualitative results

Results in Fig. 1 show a good agreement between the two codes, in particular considering how different the two models are. The shape of the interface (the volume fraction 0.5 iso-contour of for SLOSH and the Level-Set zero contour for DYJEAT) is quite similar, and the amplitude of the oscillation seems to agree, as it does the vorticity field. In spite of this, there are some hidden key aspects which it is worth to mention. In order to capture the instability without perturbations, SLOSH requires cells twice finer on the interface; at the same time its cells can become larger far from the injection, so that the total number of elements can be roughly the same. The DYJEAT solver is, in this configuration, limited in the density ratio as well as on the maximum Reynolds number (the viscosities have been increased), while SLOSH seems to be quite more robust. It has to be pointed out, however, that no strong topological changes appear in this test, situation where the Level-Set formulation should show its full potential. A parallel adaptive mesh version of DYJEAT is already running, while it seems more difficult to implement in SLOSH.

2.2.2. Quantitative results

In order to evaluate more accurately the results, a measure of the oscillation frequency has been done with both codes (see Fig. 2). The position of the sheet has been tracked in time, for many cycles, along the vertical axis, on a section of the domain located at a fixed distance from the injector. A fast Fourier transform of the resulting signal gives the best measure of the oscillation frequency. The distance from the injector has no effect on the computed frequency, only in the amplitudes (see [19] for more details). The frequency values are very similar. The conclusion is that the discrepancy with the experimental results of [3] can be explained by the difference in the physical parameters. This test confirms that primary atomization can be realistically well described by a diffuse interface method, so that its choice for the hybrid solver should be fully justified.

2.3. Primary atomization: three dimensional case

The atomization process being three dimensional, some tests were carried on to try to reproduce the full mechanism. The simulation of a truly realistic configuration is still a very difficult task for any DNS code. An effective way to test the capabilities of the code for atomization is to perform a so-called temporal simulation, where a single wavelength of the instability is followed in time while travelling into a still periodical domain (so that one looks in time what should appear in space). This simulation reveals many interesting aspects of the physics of atomization which are qualitatively well reproduced by the code. The DYJEAT code has been used in this test. These parameters are similar to the previous test in Section 2.2, and correspond to an experience realized at the ONERA LACOM laboratory of Fauga-Mauzac, done with 10 bar pressurized air and water.

The computational domain consists of a rectangular box of sides $L_x = 10a = 3$ mm, $L_y = 20a = 6$ mm and $L_z = 10a = 3$ mm, where $a = 300$ µm is the thickness of the liquid sheet. The mesh resolution is $256 \times 512 \times 256$ in the respective stream-wise (x), span-wise (y) and cross-stream (z) directions, which means around 11 µm cells. Boundary conditions are periodical in x and z directions, while free slip conditions are imposed in y. The initial condition consists of an a thick liquid

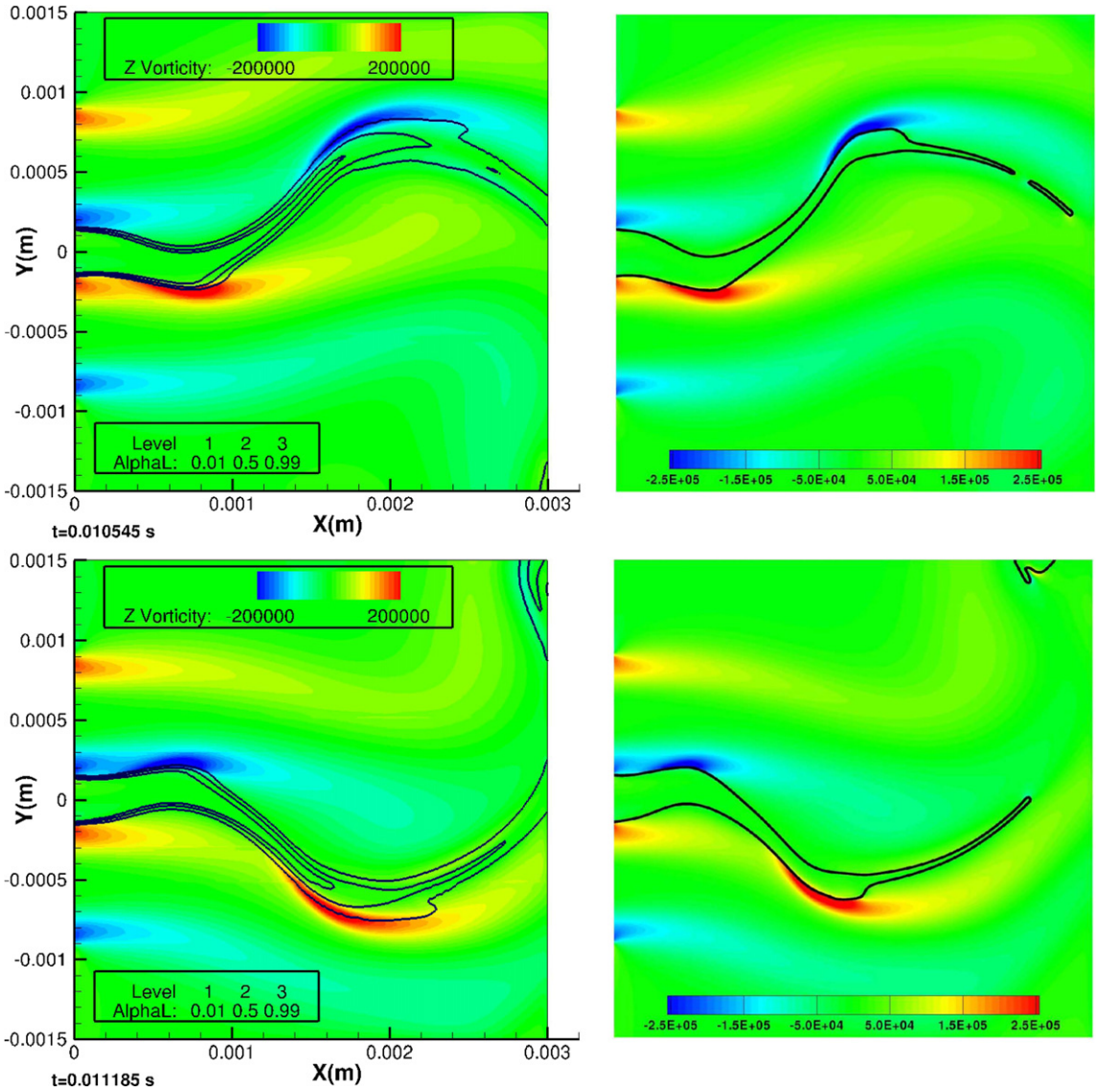

Fig. 1. Comparison of SLOSH and DYJEAT codes on the 2D atomization test case, three different instants. (Left) SLOSH, in black the contours of volume fraction at 0.25, 0.5 and 0.75. (Right) DYJEAT, in black the interface. In both the vorticity fields are depicted.[1]

sheet extending in the y-normal plane in the middle of the box. The velocity profiles are the same as the two-dimensional case, described by Eqs. (9) and (10), as well as the physical parameters.

A velocity perturbation is added, in the form:

$$v'(x,z) = A\sin(2\pi x/L_x) + B\sin(6\pi z/L_z) \tag{11}$$

which means that one period of stream-wise perturbation is given, while three periods are given in the cross-flow direction. The wavelength come from experimental results in (almost) the same conditions, given in [3].

Fig. 3(a) shows the initial condition of the liquid sheet. In the following shot (Fig. 3(b)) the instabilities start to develop, beginning the formation of the bag-like fluid structures. The downwind vortices start to scratch the liquid on the points of maximum amplitude of the sheet. Fig. 3(c) shows a clear view of both the bags and ligaments. Some of those start to break-up, thus forming the first droplets. In the last screenshot (Fig. 3(d)) the bags are gone, the dominant fluid structures are the ligament and droplets of different sizes.

[1] Note: The contour scales are slightly different on the two sets of images (max 2×10^5 on the left, 2.5×10^5 on the right), so that the SLOSH computed vorticity peaks appear a little more "smeared". Closer investigations revealed no substantial differences in computed values.

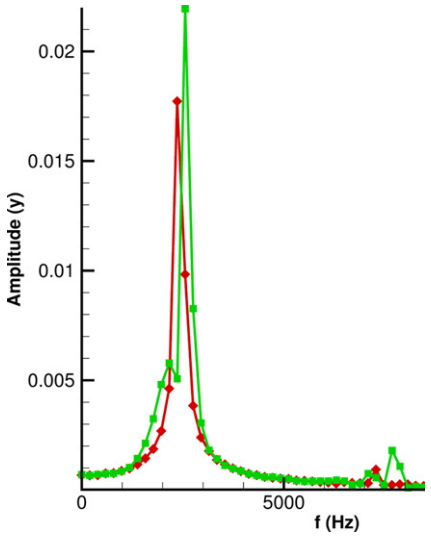

Fig. 2. Oscillation frequency of the liquid sheet in the 2D atomization test case. ■ DYJEAT, ♦ SLOSH. The peak at around 2500 Hz corresponds to the global oscillation.

Given a closer look to the sheet evolution, two important mechanisms of fragmentation can be observed, the ligament and the membrane (bag) break-up. Fig. 4 shows a starting ligament still attached to the main structure of the fragmenting sheet, the stream flowing in the positive x direction (rightwards). It separates from it by forming a sort of swelling on the down-stream side; then, the connection of this new structure stretches till the separation, where a big drop is formed. The rest of the ligament body shrinks and starts the drop formation again, now on the up-stream side.

The membrane break-up can be observed in Fig. 5, where the flow is now coming towards the observer. A hole appears in the central liquid membrane, while from the upwind limb a ligament starts to develop downwards. The hole stretches, and the membrane quickly degenerates into a set of ligaments and droplets. It is no more visible in the last image of the sequence.

3. (Hybrid) multi-fluid solver development

3.1. Presentation of the coupling strategy

A new method for simulating the whole atomization process is under development at ONERA. As introduced in Section 2, it consists in a coupling between an interfacial flow solver and a dispersed phase solver.

The interfacial flow solver is dedicated to a small part of the computational domain, near the injector, to capture large scale features of the interface and the ligament formation created during the primary atomization process. As regards the dispersed phase solver, it is dedicated to the rest of the domain where the secondary atomization process occurs (see Fig. 6(a)). A crucial point is to develop a robust coupling procedure between these solvers, which would allow to create and inject droplets from the interfacial flow solver to the dispersed phase solver.

To start the development and demonstrate its feasibility, the SLOSH solver have been chosen as the interfacial flow solver and a Lagrangian particle tracking solver have been written to act as the dispersed phase solver.

3.2. Details on the Lagrangian particle tracking solver

3.2.1. Liquid phase

The liquid phase is assumed to be a dilute spray composed of hard spherical droplets ($\rho_l/\rho_g \gg 1$), so that collisions and coalescences are neglected. The Lagrangian particle tracking solver transports droplets with a two-way coupling between the gaseous phase and the droplets. The position x_p and the velocity v_p of a droplet p, whose trajectory is only governed by the drag force, is given by (12) and (13):

$$\frac{\mathrm{d}x_p(t)}{\mathrm{d}t} = v_p(t) \tag{12}$$

$$\frac{\mathrm{d}v_p(t)}{\mathrm{d}t} = \frac{u_{g@p}(t) - v_p(t)}{\tau_p} \tag{13}$$

where $u_{g@p}$ is the gas velocity interpolated at the droplet location and τ_p is the droplet relaxation time. The expression of τ_p is [20]:

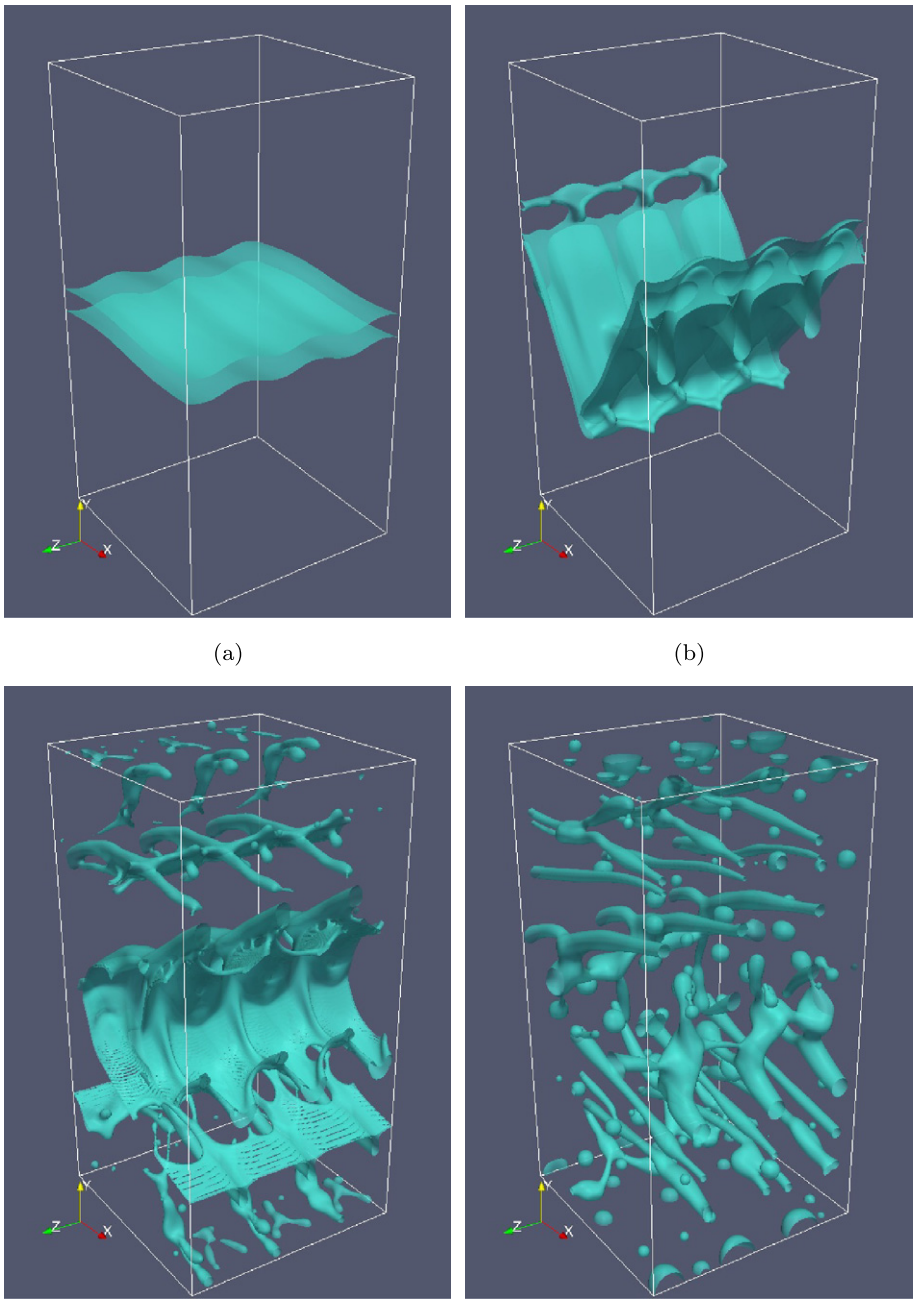

Fig. 3. Results from high resolution liquid sheet disintegration, primary and secondary atomization. Ligament break-up and formation of the droplets.

$$\tau_p = \frac{d_p^2 \rho_p}{18 \nu_{g@p} \rho_{g@p}} \left[1 + 0.15\, \mathcal{R}e_p^{0.687}\right]^{-1} \tag{14}$$

where the Reynolds number based on the droplet diameter d_p is:

$$\mathcal{R}e_p = \frac{\rho_{g@p} d_p |u_{g@p} - v_p|}{\mu_{g@p}} \tag{15}$$

As regards the numerical implementation, a parcel formulation is used to avoid an excessive computational cost: instead of tracking individually N_p droplets, only N_c ($N_c < N_p$) computational particles are used. Each computational particle represents statistically a cloud of droplets with similar physical properties and characteristics. The numbers N_c and N_p verify:

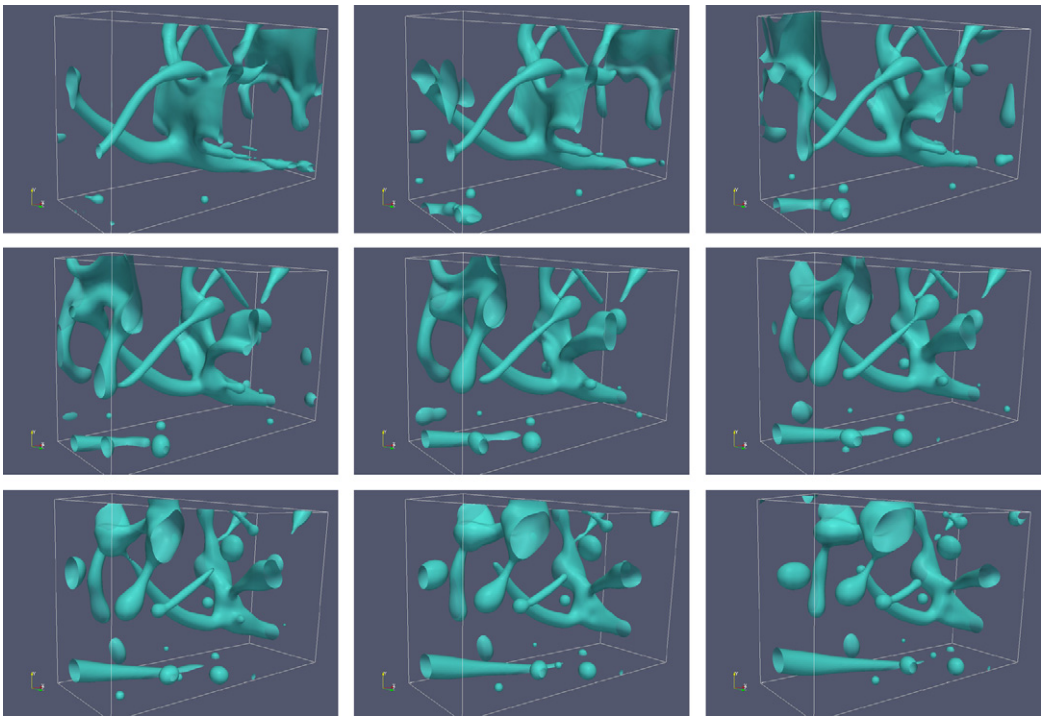

Fig. 4. Detail of the three-dimensional simulation, ligament break-up. Screenshots should be read from left to right, top to bottom.

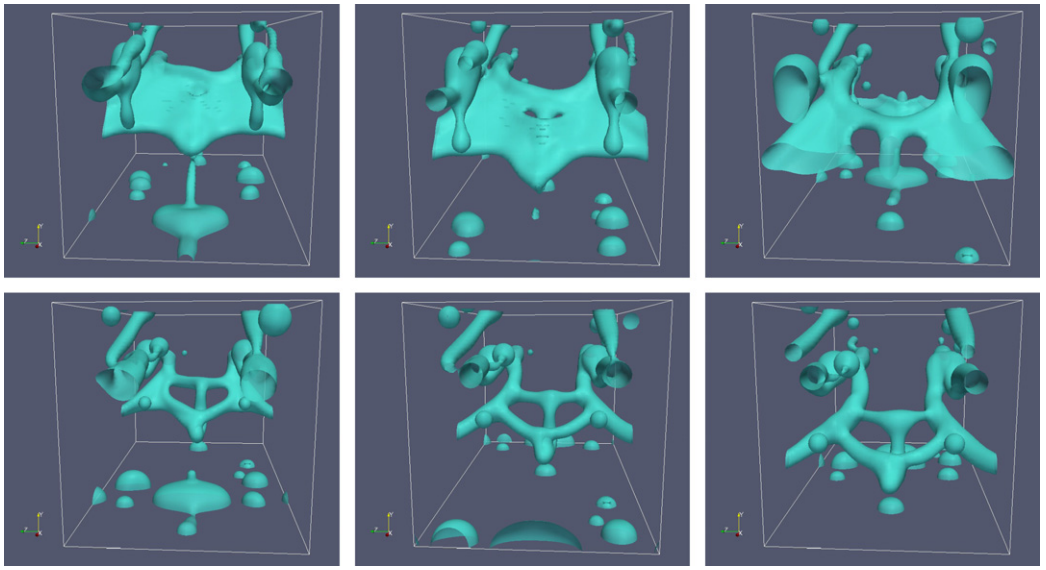

Fig. 5. Detail of the three-dimensional simulation, bag break-up. Screenshots should be read from left to right, top to bottom.

$$N_p = \sum_{i=1}^{N_c} w_c(i) \tag{16}$$

where $w_c(i)$ is the statistical weight of the computational particle i.

3.2.2. Gaseous phase

The SLOSH solver is degenerated into a monofluid solver to solve the gaseous phase. Besides, to ensure a two-way coupling between droplets and the gaseous phase, a source term S_{Lag} is added in the right side of the momentum equation of the gas (see (17)). The expression of this source term is given by (18).

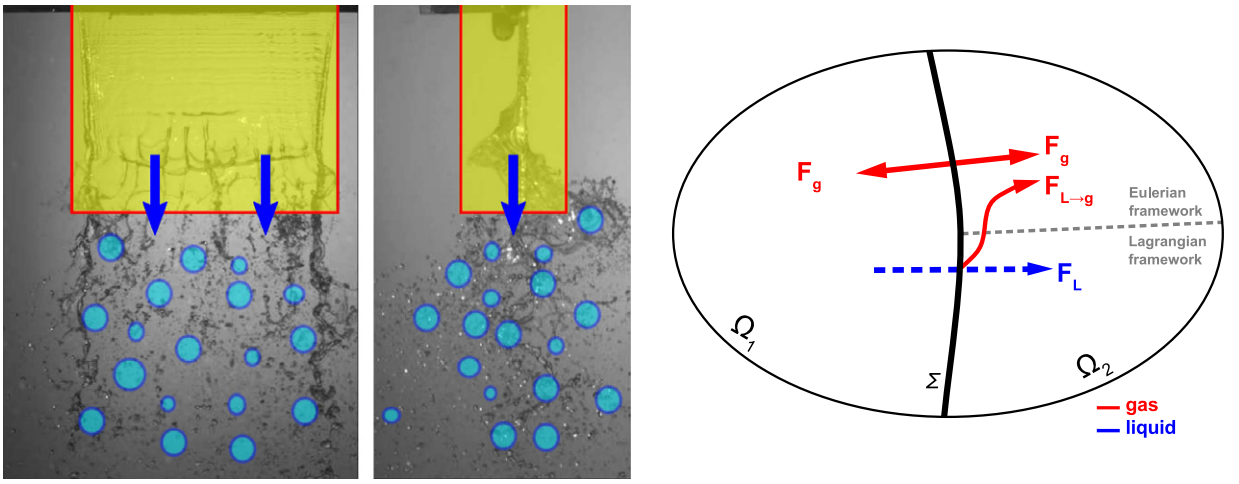

Fig. 6. Hybrid solver for atomization simulation. (a) Domains of competence of each solver: multi-fluid for the inner region and dispersed phase for the outer region, and the interface Σ between. (b) Numerical fluxes exchange between solvers at the interface Σ.

$$\frac{\partial}{\partial t}(\rho_g u_g) + \nabla.(\rho_g u_g \otimes u_g + pId - \tau_D) = S_{Lag} \tag{17}$$

$$S_{Lag} = -\frac{1}{\mathcal{V}} \sum_{p\in[1;N_c]|x_p\in\mathcal{V}} \left[w_c(p) m_p \frac{\mathrm{d}v_p}{\mathrm{d}t} \right] \tag{18}$$

where $\mathcal{V}$ is the element of volume of the domain.

3.3. Coupling procedure

The coupling between the Eulerian multi-fluid solver and the Lagrangian particle tracking solver is achieved at the interface Σ, depicted in Fig. 6(b).

At the present time, this interface Σ is composed of an user-defined set of adjacent faces of the meshing, which makes this method easy to implement in the finite volume approach of the SLOSH solver. However, to optimize the location of the interface Σ, it is necessary to know where the transition between the primary and the secondary atomization processes occurs. For this reason, developments are planned to develop criteria, based on the interface topology of the liquid phase captured by the multi-fluid solver, which will allow to adapt automatically the location of interface Σ during the simulation.

One possible criterion could be based on the break-up length of the sheet. This value is defined as the distance from the injector lips to the end of the injected liquid as a continuous body. In order to measure this length, it could possible to employ a propagating tagging algorithm to identify the cells contained in the liquid main body.

A specific treatment is performed of the liquid and gas fluxes through the interface Σ. In particular, the flux F_L of the liquid phase which goes from the multi-fluid solver to the Lagrangian particle tracking solver through the faces of Σ is transformed in computational particles. To create each computational particle, it is necessary to determine its characteristics (position, velocity, size and statistical weight). The position of the particle is chosen randomly on the face of Σ where the flux F_L is considered. The diameter of the droplet is chosen according to a log-normal law whose parameters are user-defined at the present time. Then, the velocity and the statistical weight are calculated such as the mass and the momentum of the liquid phase are conserved. As regards the gas phase, an additional flux $F_{L\to g}$ of gas is injected in the multi-fluid solver to compensate for the volume of the droplets that is not explicitly taken into account in the Lagrangian framework. The expression of the flux $F_{L\to g}$ is:

$$F_{L\to g} = \frac{\rho_g}{\rho_L} F_L \tag{19}$$

where F_L is the liquid flux leaving the multi-fluid solver through Σ.

3.4. First results

The same test case as in Section 2.2 was carried out, the liquid sheet atomization in two dimensions. The region inside the interface Σ (the multi-fluid solver) corresponds to the whole simulation in Section 2.2, with the same configuration and parametrization; outside Σ the domain has been extended and solved by the Lagrangian solver.

The simulation (Fig. 7) has been performed in two steps:

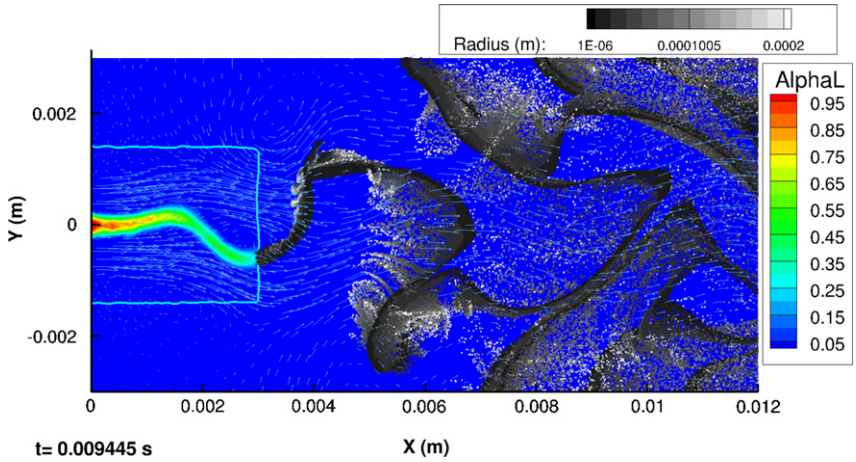

Fig. 7. Two dimensional atomization of a liquid sheet with hybrid solver. The sky-blue rectangle corresponds to the interface Σ. Inside Σ the two-fluid SLOSH is active, the colour representing the liquid concentration; outside the degenerated gas-only version of SLOSH performs the transport of the droplets, created at the interface to match the outgoing liquid flux.

- ▹ a transitory where the continuous phase solver only is active in both the domains;
- ▹ an established regime where the two models are active in their respective domain.

The results are qualitative but show clearly the capabilities of the model. The droplets are created following the oscillation movement of the sheet, and the behaviour of the droplet cloud agrees with similar test cases like [16]. The transfer of flux across Σ seems to be correct, as no perturbation of the liquid motion is visible outside the global oscillation. The droplet diameter distribution is arbitrary fixed, but a model which takes into account the sheet topology will be introduced in the future.

4. Conclusion

An overview of the different ways to perform atomization simulation at ONERA has been given. Two research codes make use of different approaches for two-phase flows, and give good result in the presented test cases. On the other hand, in order to efficiently perform full three-dimensional assisted atomization simulations a new model seems necessary to correctly take into account the physics underlying the different moments of atomization. The investigation of the different techniques of numerical simulation of multi-phase flows led to the definition of the model which is planned to be integrated into the ONERA CEDRE code. The atomization multi-scale nature make the choice to fall on an hybrid solver, composed of an Eulerian multi-fluid solver for the primary atomization and a dispersed phase solver for the secondary atomization, two of them being already available in CEDRE.

The experience given by the SLOSH code indicates that a diffuse interface method for the multi-fluid solver seems to be the most suitable to the unstructured mesh and compact finite volume formulation of CEDRE. The more precise sharp interface methods may reveal too complex and not flexible enough to be used in this context, so that they will be put aside unless absolute necessity would arise. The Navier–Stokes solver of CEDRE is able to deal with a multi-species flows by replacing the total mass conservation equation by the mass conservation equations of each specie. Hence, an extension to multi-species multi-phase model can be obtained by declaring to which fluid the species belong to, and by adding the capillarity effects.

The development of the new methods is carried on with the SLOSH code, and preliminary results are encouraging. The liquid mass flux leaving the multi-fluid solver has successfully been converted in droplets, without any visible artificial alteration of the gas motion.

References

[1] A. Aliseda, E.J. Hopfinger, J.C. Lasheras, D.M. Kremer, A. Berchielli, E.K. Connolly, Atomization of viscous and non-Newtonian liquids by a coaxial, high-speed gas jet. Experiments and droplet size modeling, International Journal of Multiphase Flow 34 (2008) 161–175.
[2] D. Kim, O. Desjardins, M. Herrmann, P. Moin, Toward two-phase simulation of the primary breakup of a round liquid jet by a coaxial flow of gas, Technical report, Annual Research Briefs, Center for Turbulence Research, 2006.
[3] Vital Gutierrez Fernandez, Experimental study of a liquid sheet disintegration in a high pressure environment, PhD thesis, ISAE, 2009.
[4] R. Lebas, T. Menard, P.A. Beau, A. Berlemont, F.X. Demoulin, Numerical simulation of primary break-up and atomization: DNS and modelling study, International Journal of Multiphase Flow 35 (2009) 247–260.
[5] O. Desjardins, V. Moureau, H. Pitsch, An accurate conservative level set/ghost fluid method for simulating turbulent atomization, Journal of Computational Physics 227 (18) (2008) 8395–8416.
[6] Marcus Herrmann, Detailed numerical simulations of the primary atomization of a turbulent liquid jet in crossflow, Journal of Engineering for Gas Turbines and Power 132 (6) (2010) 451–466.

[7] G. Tomar, D. Fuster, S. Zaleski, S. Popinet, Multiscale simulations of primary atomization using Gerris, Computers and Fluids 39 (10) (2010) 1864–1874.
[8] D. Fuster, A. Bagué, T. Boeck, L. LeMoyne, A. Leboissetier, S. Popinet, P. Ray, R. Scardovelli, S. Zaleski, Simulation of primary atomization with an octree adaptive mesh refinement and VOF method, International Journal of Multiphase Flow 35 (2009) 550–565.
[9] S. Apte, M. Gorokhovski, P. Moin, LES of atomizing spray with stochastic modeling of secondary break-up, International Journal of Multiphase Flow 29 (2003) 1503–1522.
[10] M.A. Gorokhovski, V.L. Saveliev, Analyses of Kolmogorov's model of breakup and its application into Lagrangian computation of liquid sprays under air-blast atomization, Physics of Fluids 15 (1) (2003) 184–192, http://dx.doi.org/10.1063/1.1527914.
[11] M. Herrmann, A parallel Eulerian interface tracking/Lagrangian point particle multi-scale coupling procedure, Journal of Computational Physics 229 (2010) 745–759.
[12] X. Li, M. Arienti, M. Soteriou, M. Sussman, Towards an efficient, high-fidelity methodology for liquid jet atomization computations, in: 48th AIAA Aerospace Sciences Meeting, 2010, AIAA 2010-210.
[13] Frédéric Couderc, Développement d'un code de calcul pour la simulation d'écoulements de fluides non miscibles. Application à la désintégration assistée d'un jet liquide par un courant gazeux, PhD thesis, ENSAE, 2007.
[14] N. Shied, J.-P. Vila, P. Villedieu, Programme compere – développement d'un schéma bas Mach dans le code slosh, Technical Report RF 2/14018, ONERA/DMAE, Mars 2009.
[15] N. Grenier, P. Villedieu, J.-P. Vila, An accurate low-Mach scheme for a compressible two fluid model applied to sloshing phenomena, in: Proceedings of ASME–JSME–KSME Joint Fluids Engineering Conference, AJK2011-FED, Hamamatsu, Shizuoka, Japan, July 24–29, 2011.
[16] D. Zuzio, Direct numerical simulation of two phase flows with adaptive mesh refinement, PhD thesis, ISAE, 2010.
[17] G. Chanteperdrix, Modélisation et simulation numérique d'écoulements diphasiques interface libre. Application l'étude des mouvements de liquides dans les réservoirs de véhicules spatiaux, PhD thesis, ISAE, 2004.
[18] G. Blanchard, Couplage de modèles et de méthodes numériques pour la simulation de l'atomisation d'un jet liquide, Technical report, ONERA, 2011.
[19] D. Zuzio, J.-L. Estivalezes, A parallel adaptive projection method for incompressible two phase flows, in: Computational Fluid Dynamics 2010. Proceedings of the Sixth International Conference on Computational Fluid Dynamics, ICCFD6, St Petersburg, Russia, July 12–16, 2010, Springer, 2010, URL: http://download.springer.com/static/pdf/917/bfm%253A978-3-642-17884-9%252F1.pdf?auth66=1354399748_748c2d37a85547f1117baafafe89e65c&ext=.pdf.
[20] C.T. Crowe, M. Sommerfeld, Y. Tsuji, Multiphase Flows with Drops and Particles, CRC Press, 1998.